Effects of Passivation Layer on Stress Relaxation and Mass Transport in Electroplated Cu Films

Dongwen Gan[*], Rui Huang[#], Paul S. Ho[*],
Jihperng Leu[+], Jose Maiz[+], and Tracey Scherban[+]

[*]*Laboratory for Interconnect & Packaging, University of Texas, Austin, TX 78712*

[#]*Aerospace Engineering & Engineering Mechanics Department, University of Texas, Austin, TX 78712*

[+]*Intel Corporation, Hillsboro, OR 97214*

Abstract. Recent studies have shown that the Cu/cap layer interface is the dominant diffusion path for electromigration (EM) in Cu interconnects, making it important to develop effective methods to evaluate the effect of passivation layer on interfacial mass transport and EM lifetime for Cu interconnects. This work shows that a set of isothermal stress relaxation tests together with appropriate modeling analysis can be used to evaluate the kinetics of interface and grain boundary diffusion and the effects of passivation layer. Thermal stresses in electroplated Cu films with and without passivation were measured using a bending beam technique, subjected to thermal cycling and isothermal annealing at selected conditions. Thermal cycling experiments provide information to select the initial stresses and temperatures for isothermal stress measurements. A kinetic model coupling grain boundary diffusion with surface and interface diffusion was developed and found to account well for the isothermal stress relaxation experiments within a certain range of temperatures and stresses. Based on the kinetic model, both the grain boundary diffusivity and the Cu/SiN interface diffusivity were deduced from isothermal stress relaxation measurements. While the deduced grain boundary diffusivity reasonably agrees with other studies, the diffusivity at the Cu/SiN interface was found to be considerably lower than the grain boundary diffusivity within the temperature range of the present study.

INTRODUCTION

The formation of Cu damascene interconnect structures requires complex processes and structural elements, including electroplating Cu, barrier/seed layers, chemical-mechanical polishing (CMP) and passivation. Recent studies showed that these processes and elements give rise to distinct defect characteristics and mass transport paths, leading to failure mechanisms of electromigration (EM) and stress voiding for Cu interconnects different from Al interconnects. In particular, electromigration studies in Cu line structures showed that mass transport is dominated by diffusion at the Cu/cap layer interface, probably due to the presence of defects

induced by CMP [1, 2]. This raises the possibility of reducing interfacial mass transport to improve EM lifetime by optimization of the chemical bonds at the Cu/cap layer interface. Recently, Lane et al. [3] showed that EM lifetime of Cu interconnects can indeed be improved by optimizing the interfacial bond using different cap layers and cleaning processes, and their results were supported by a correlation between EM lifetime and interfacial adhesion. This was corroborated by Hu et al. [4] who demonstrated a significant improvement in EM lifetime by coating the Cu surface with a thin (20-30nm) metal layer.

As interconnect scaling advances beyond the 90 nm node, the interface to volume ratio continues to increase with decreasing line width, making interfacial diffusion increasingly important in contributing to mass transport and thus in controlling the EM reliability of Cu interconnects. To evaluate the effect of passivation layer on interfacial mass transport and EM lifetime for Cu interconnects, we developed a bending beam technique to measure isothermal stress relaxation in Cu films and line structures. This method has been applied to measure the cap-layer effect on interfacial mass transport in Cu damascene lines with results found to be consistent with EM and adhesion measurements [5]. In this paper, we report the results obtained from a stress relaxation study of electroplated Cu films with and without a passivation layer, which clearly shows the effect of passivation on mass transport in electroplated Cu films. A coupled diffusion model was developed to quantitatively correlate isothermal stress relaxation with the kinetics of mass transport through interface and grain boundaries. By combining the stress relaxation measurements and the diffusion model, the grain boundary and interface diffusivities of the Cu films were deduced. Results from this study demonstrate that isothermal stress relaxation measurement is an effective method to evaluate the interfacial mass transport in Cu metallization.

EXPERIMENTAL

A. Sample Preparation and Stress Measurement

Cu film samples were prepared on silicon wafers with 200nm thermal oxide (TEOS) on both sides. A layer of silicon nitride (SiN) was deposited on one side of the wafer by a CVD process, followed by the deposition of a diffusion barrier layer to prevent the Cu atoms from diffusing into the substrate. A Cu seed layer of 100 nm thick was then deposited on the barrier layer by a PVD process. The rest of the Cu film was prepared by an electroplating process and the total thickness of the Cu film was 1.0 μm. Some films were further capped with 50nm SiN and 200 nm silicon oxide as passivation.

Stress in the Cu films was measured using a bending beam system developed in our laboratory [6], which determines the stress in a film by measuring the curvature change of the substrate. The stress in a film with a thickness much less than that of the substrate can be calculated using Stoney's equation,

$$\sigma = \frac{E_s h_s^2}{6(1-\nu_s)h}\left(\frac{1}{R} - \frac{1}{R_0}\right), \quad (1)$$

where σ is the film stress, E_s the Young's modulus of the substrate, ν_s the Poisson's ratio of the substrate, h_s the substrate thickness, h the film thickness, R the radius of the curvature of the substrate with the film, and R_0 the radius of the curvature of a bare substrate. For the passivated Cu films, the contribution to the curvature change from the oxide passivation layer was accounted for by using the stress of a bare silicon oxide film on a Si substrate as the reference. The contribution from the SiN layer was ignored since its thickness is much smaller than that of the Cu film. The radius R_0 was measured after the film was etched off. The relocation of the sample beams and other uncertainties would induce a system error estimated to be about 5%.

The samples were cut into 5mm by 40mm stripes. The surface curvatures were monitored and recorded as the samples were thermally loaded in a vacuum chamber under a nitrogen atmosphere at a pressure of 50 torr. In this study, stresses in the Cu films were first measured under thermal cycles, and then isothermal stress relaxation tests were performed at the selected temperatures.

B. Stress under Thermal Cycling

Figure 1(a) shows the measured stress behavior of a passivated and an unpassivated Cu film in two thermal cycles with different ramping rates. In the 1st cycle (not shown in the figure), the temperature range was from room temperature (RT) to 460ºC where the films were annealed for 30 minutes to stabilize their microstructures. Subsequently, the temperature cycles from RT to 450ºC with the ramping rates of 1.5ºC/min and 6ºC/min. In each cycle, upon initial heating, the stress in both films decreased linearly with temperature but then deviated from the elastic behavior with the onset of plastic deformation. Further increasing of temperature resulted in the change of stress from tension to compression with increasing plastic deformation. Upon cooling, the compressive stress decreased and then changed back to be tensile and reached the initial stress at the room temperature, leaving a hysteresis loop as an evidence of plastic deformation in the film. It is noted that the shape of the stress-temperature curves for the electroplated Cu films in the present study is different from those for e-beam and sputtering deposited Cu films [7-9], which indicates an effect of the deposition process on the thermomechanical behavior of Cu films.

Compared to the unpassivated film, the passivated film had a higher tensile residual stress at RT and reached a higher compressive stress at high temperatures, which clearly shows the effect of passivation on the stress behavior under thermal cycling. On the other hand, the stress hysteresis shows no noticeable difference as the ramping rate changed from 6ºC/min to 1.5ºC/min. This suggests that the dominant process of the plastic deformation during thermal cycling takes place at a rate much faster than the ramping rates, similar to plastic yielding at low temperatures under conventional mechanical tests. At high temperatures, it was expected that diffusional creep as a

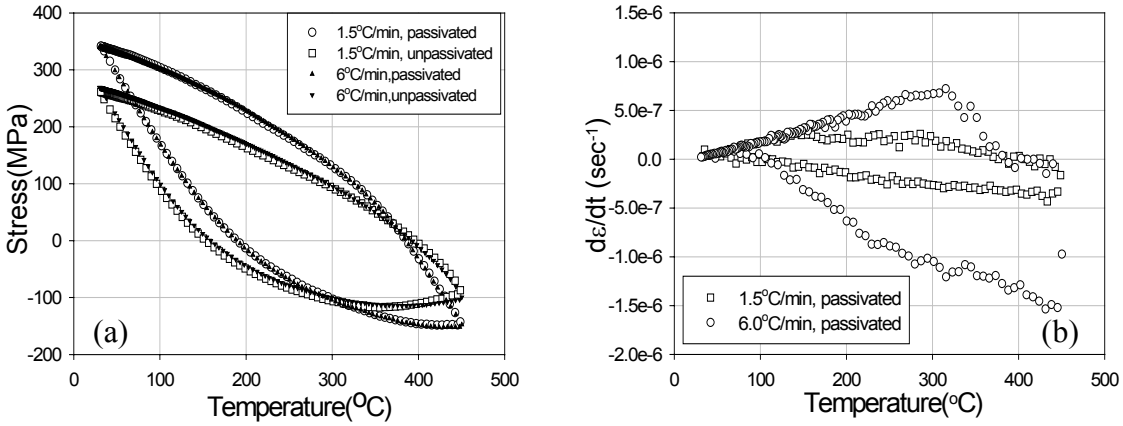

FIGURE 1. (a) Stress behavior of Cu films, passivated and unpassivated, in thermal cycles with different ramping rates; (b) Deduced plastic strain rate of the passivated Cu film in the thermal cycles.

result of mass transport would contribute to stress relaxation. However, no significant difference was observed in the stresses for temperatures up to 450ºC, which implies that, within the range of the ramping rates, the contribution from diffusional creep is negligible. In a separate study [10], we observed more stress relaxation at high temperatures when the ramping rate was reduced to 0.5ºC/min. Therefore, the stress relaxation process may consist of a fast process upon loading due to plastic yielding and subsequently a slow process due to diffusional creep. Except for very slow ramping rates, the fast process dominates in the thermal cycling experiments, making it difficult to extract any information about diffusional creep and the associated mass transport. The effect of the cap layer observed under thermal cycling is thus most likely due to the confinement effect on plastic yielding [11], rather than on mass transport.

Figure 1(b) shows the plastic strain rate of the passivated Cu film deduced from the stress-temperature curves. It clearly shows that the plastic strain rate, averaged over each time interval of temperature ramping [10], strongly depends on the ramping rate. Any steady-state deformation mechanism would thus be unable to account for such behavior. The decrease of the strain rate upon cooling below a particular temperature was found to correlate to the decrease of the ramping rate as it could not be held constant in the experiments. For both the passivated and unpassivated Cu films, it was found that the plastic strain rate is approximately proportional to the ramping rate. While such strain rate provides no obvious connection to the kinetics of mass transport, the measured stress under thermal cycling may be considered as the "yield strength" of the film, which is independent of the ramping rate but is a function of the temperature and the accumulated plastic strain.

C. Isothermal Stress Relaxation

The stress hysteresis obtained from the thermal cycling experiments provides information to select the initial stresses and temperatures for isothermal stress

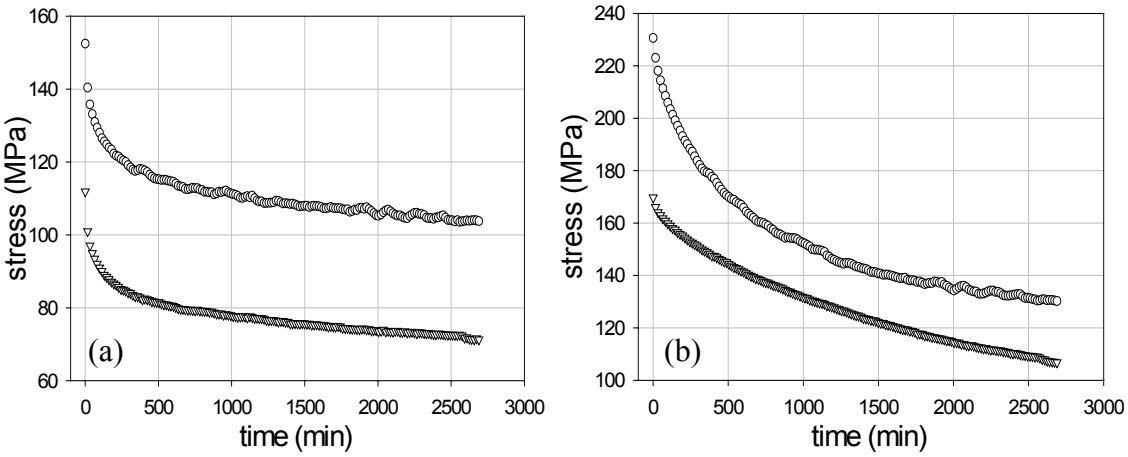

FIGURE 2. Isothermal stress relaxation of Cu films from different initial stresses at 200ºC: (a) unpassivated Cu film, and (b) passivated Cu film.

relaxation measurements, which is more suited for the study of mass transport. By varying the peak temperature of thermal cycling, one can adjust both the temperature and the initial stress for isothermal measurements to separately investigate the effect of stress and temperature on mass transport. The hysteresis loop of the stress-temperature curves can be roughly divided into four regimes: a low-temperature elastic regime upon heating, an inelastic regime under compression, a high-temperature elastic regime upon cooling, and an inelastic regime under tension. Each of these regimes may be associated with different deformation and mass transport mechanisms [8, 12]. In particular, we found that the stress relaxation behavior with a compressive initial stress is quite different from that with a tensile initial stress, even at the same temperature. In this study, we focused on stress relaxation at selected temperatures with initial tensile stresses.

Figure 2 shows the measured stress relaxation curves of the unpassivated and passivated Cu films starting from different initial stresses at 200ºC for 45 hours. The initial stresses for the passivated film are about 231MPa and 170MPa, and those for the unpassivated film are 152MPa and 112MPa. The higher initial stresses were achieved by cooling the films from 450ºC, and the lower ones from 350ºC in the 2nd cycle. A higher initial stress resulted in more stress relaxed within the period of 45 hours but still retained a higher stress at the end for both the passivated and unpassivated films. Each curve shows an initial stage of sharp decrease of stress with time (especially for the unpassivated film) and then a steady stress relaxation over a long period. The plastic strain rates deduced from Fig. 2 are shown in Fig. 3 as functions of the stress. The significance of the transient behavior at the initial stage is clearly observed from Fig. 3 for both the unpassivated and the passivated films. Each curve in Fig. 3 can be roughly divided into an initial transient regime and a steady state regime, a typical behavior of creep [13]. Within the transient regime, the plastic strain rate not only depends on the current stress but also depends on the stress history or, in particular, the initial stress and the time since the relaxation started. As the

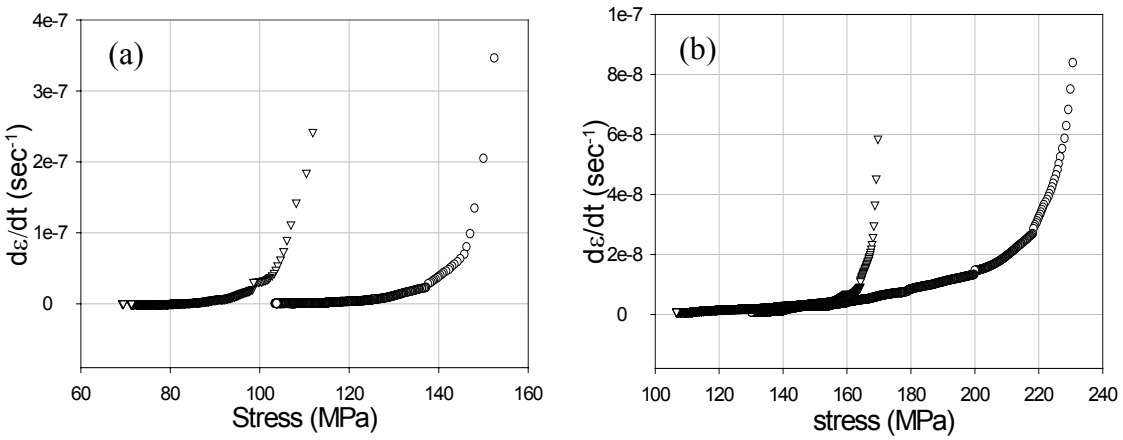

FIGURE 3. Plastic strain rate as a function of stress in isothermal stress relaxation at 200ºC for (a) the unpassivated Cu film and (b) the passivated Cu film.

starting point of the stress relaxation measurements were taken from thermal cycling experiments, this confirms that, under the thermal cycling, the films had not reached the steady state and the effect of the transient behavior is significant. On the other hand, isothermal stress relaxation tests measured stress evolution over a long period, allowing detailed analyses of the kinetics from the transient regime to the steady state. In particular, we note that, compared to the unpassivated Cu film, the passivated Cu film started with a lower strain rate even though the stress was higher, most likely due to the effect of the passivation on the diffusion processes.

MODELING AND ANALYSIS

A. A Coupled Diffusion Model

To quantitatively correlate the measured stress relaxation data to the kinetics of mass transport, we developed a coupled diffusion model. Figure 4 schematically illustrates the structure and diffusion paths in unpassivated and passivated thin films, where the film ideally consists of one layer of grains with the grain boundaries perpendicular to the film-substrate interface. For an unpassivated film, stress is relaxed by diffusional flow of matter between the free surface and the grain boundaries. Similarly, in a passivated film, mass transport at the interface between the film and the cap layer contributes to the stress relaxation. In both cases, the mass transport at the film/substrate interface is assumed to be negligible.

At the free surface of an unpassivated film, the chemical potential is proportional to the local curvature. The gradient of the chemical potential drives surface diffusion and the evolution of the surface profile. The equation governing the surface diffusion is identical to that by Mullins [14] in the original analysis of grain-boundary grooving, i.e.,

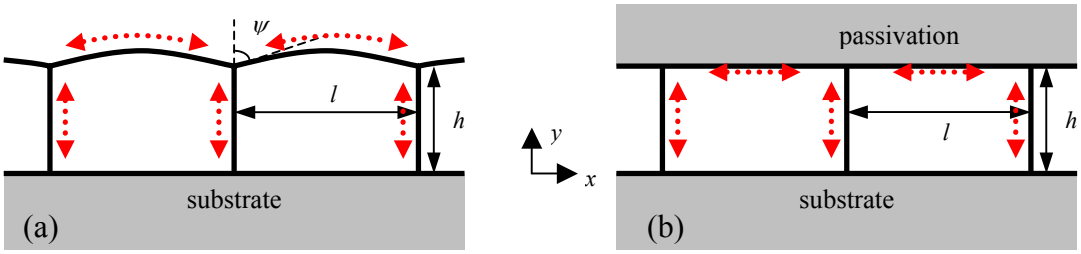

FIGURE 4. Schematics of polycrystalline thin films: (a) an unpassivated film; (b) a passivated film.

$$\frac{\partial \bar{y}}{\partial t} = -\frac{\delta_S D_S \gamma_S \Omega}{kT} \frac{\partial^4 \bar{y}}{\partial x^4}, \tag{2}$$

where $\bar{y}(x,t)$ represents the surface profile, δ_S is the thickness of the surface layer, D_S is the surface diffusivity, γ_S is the surface energy density, Ω is the atomic volume, k is Boltzmann's constant, and T is the absolute temperature.

At a grain boundary, the chemical potential is proportional to the normal stress. The distribution of the normal stress evolves as atoms diffuse along the grain boundary. The divergence of mass transport at the grain boundary induces an inelastic strain (or creep strain), which, by a linear spring model [15], is related to the rate of the grain boundary stress. In terms of the normal stress, the governing equation for the grain-boundary diffusion is then

$$\frac{\partial \sigma_B}{\partial t} = \frac{M\Omega\delta_B D_B}{lkT} \frac{\partial^2 \sigma_B}{\partial y^2}, \tag{3}$$

where $\sigma_B(y,t)$ is the normal stress at the grain boundary, δ_B is the width of the grain boundary, D_B is the grain boundary diffusivity, M is the elastic modulus of the film, and l is the grain size.

For a passivated film, we define a chemical potential at the interface between the film and the cap layer proportional to the local normal stress, similar to that at a grain boundary. The total resultant force at the interface, however, vanishes as required by equilibrium. The mass insertion or removal at the interface due to divergence of the atomic flux can be accommodated by a combination of the grain deformation and a rigid body motion of the cap layer. Assuming elastic grains (similar to the linear spring model for the grain boundary stress [15]) and a rigid cap layer, we obtain that

$$\frac{\partial \sigma_I}{\partial t} = \frac{M\Omega\delta_I D_I}{hkT} \frac{\partial^2 \sigma_I}{\partial x^2} + \frac{2M\Omega}{hl} J_0(t), \tag{4}$$

where $\sigma_I(x,t)$ is the local normal stress at the interface, δ_I is the thickness of the interface layer, D_I is the interface diffusivity, and $J_0(t)$ is the atomic flux rate at the junction between the interface and a grain boundary.

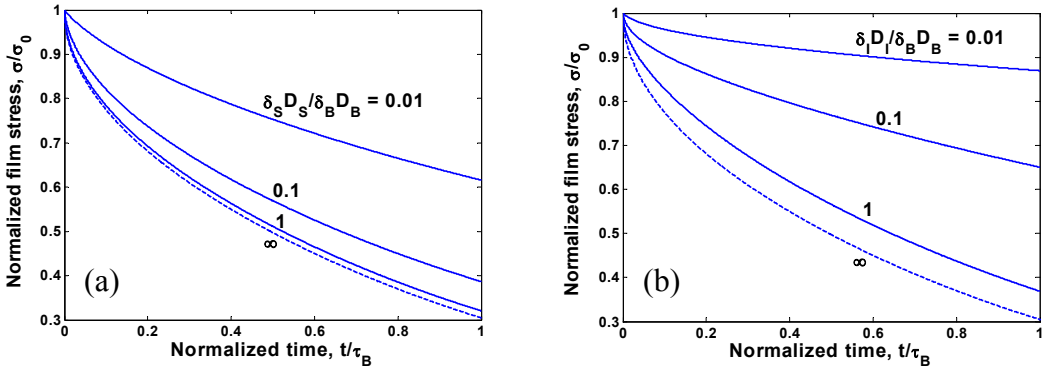

FIGURE 5. Effects of (a) surface diffusivity and (b) interface diffusivity on stress relaxation of unpassivated and passivated films, respectively.

The mass transport processes are coupled as the chemical potential and the atomic flux are required to be continuous at the junction between a grain boundary and the surface or interface. Additional boundary conditions are specified by assuming no flux at the film/substrate interface and a periodic grain structure. The coupled problem can then be solved numerically. The effective stress of the film was determined by the average of the normal stress along the grain boundary. Consequently, the relaxation of the film stress depends on the kinetics of the mass transport processes. Figure 5 shows the predicted stress relaxation in unpassivated and passivated films with different ratios between the diffusivities, where the stress is normalized by the initial stress and the time is normalized by a time scale characterizing the grain boundary diffusion

$$\tau_B = \frac{4kTh^2 l}{\pi^2 M\Omega\delta_B D_B}. \tag{5}$$

Figure 5(a) shows that, for unpassivated films, the stress relaxation curve is insensitive to the surface diffusivity as long as surface diffusion is faster than grain boundary diffusion. In such cases, the surface diffusion may be approximately taken to be infinitely fast, for which a closed form solution was obtained:

$$\sigma(t) = \sigma_\infty + (\sigma_0 - \sigma_\infty)\frac{8}{\pi^2}\sum_{n=0}^{\infty}\frac{\exp\left[-(2n+1)^2 t/\tau_B\right]}{(2n+1)^2}, \tag{6}$$

where σ_0 is the initial stress and σ_∞ is the zero-creep stress [13]. The close form solution is plotted in Fig. 5(a) as the dashed line. Equation (6) consists of a series expansion with each term decaying exponentially with time, similar to that obtained by Gao et al. [16], but with different time scales. While a steady-state linear creep leads to stress relaxation with one exponential term, the multitude of the exponential terms in Eq. (6) predicts a transient behavior at the initial stage.

Figure 5(b) shows the effect of interface diffusivity on stress relaxation of passivated films predicted by the present model. Comparing to Fig. 5(a), the stress relaxation is much more sensitive to the interface diffusivity for passivated films than it is to the surface diffusivity for unpassivated films, especially if the diffusivities

follow the general trend, $\delta_S D_S > \delta_B D_B > \delta_I D_I$. The sensitivity of the stress relaxation to interface diffusion allows quantitative characterization of the kinetics of mass transport along the interface, which can then be used to evaluate selected passivation layers for improving electromigration reliability of Cu interconnects. A closed form solution can also be obtained for the limiting case when the grain boundary diffusion is much faster than the interface diffusion:

$$\sigma_B(t) = \sigma_0 \frac{8}{\pi^2} \sum_{n=0}^{\infty} \frac{\exp\left[-(2n+1)^2 t/\tau_I\right]}{(2n+1)^2}, \tag{7}$$

where $\tau_I = \dfrac{kThl^2}{\pi^2 M\Omega\delta_I D_I}$ is the time scale for interface diffusion. A zero-creep stress may also be included in Eq. (7) in a similar manner as in Eq. (6). By comparing with the numerical solutions, we found that Eq. (7) is a good approximation when $\delta_B D_B > 100\delta_I D_I$.

B. Extraction of Grain Boundary and Interface Diffusivities

By using the coupled diffusion model, grain boundary and interface diffusivities can be extracted from the isothermal stress relaxation data. The corresponding activation energies can then be deduced from the temperature dependence of the diffusivities. The procedure is illustrated as follows.

First, the grain boundary diffusivity at various temperatures can be obtained from the stress relaxation curves of unpassivated films by comparing to the model prediction, i.e., Eq. (6) under the assumption that surface diffusion is typically faster than grain boundary diffusion. The zero-creep stress, σ_∞, however, is not well understood. The model predicts a negligible zero-creep stress for Cu films of 1.0 μm thickness [13], while the experimental data suggests a significant zero-creep stress. For this reason, we first deduced the zero-creep stress by an empirical fitting with two exponential terms and a third term for the zero-creep stress [10]. Then, the grain boundary diffusivity is varied to minimize the fitting error between Eq. (6) and the experimental data by means of a least square optimization. Figure 6(a) shows the stress relaxation curves at three different temperatures, 176ºC, 200ºC and 215ºC, and the fitting results. The grain boundary diffusivities ($\delta_B D_B$) of the Cu film were deduced to be 9.5e-27 m^3/s, 5.5e-26 m^3/s and 8.1e-26 m^3/s, respectively. The three diffusivities were then fitted into an Arrhenius plot as shown in Fig. 6(b), assuming $\delta_B D_B = \delta_B D_{B0} \exp(-Q_B/kT)$, from which we obtain the activation energy and the pre-exponential factor for the grain boundary diffusion: Q_B = 1.07eV and $\delta_B D_{B0}$ = 1.1 × 10^{-14} m^3/s. Table 1 lists the other parameters for the Cu film as well as the deduced grain-boundary diffusivity and the activation energy.

Next, the interface diffusivities at various temperatures are deduced similarly from the stress relaxation curves for the passivated Cu film by varying the ratio between the

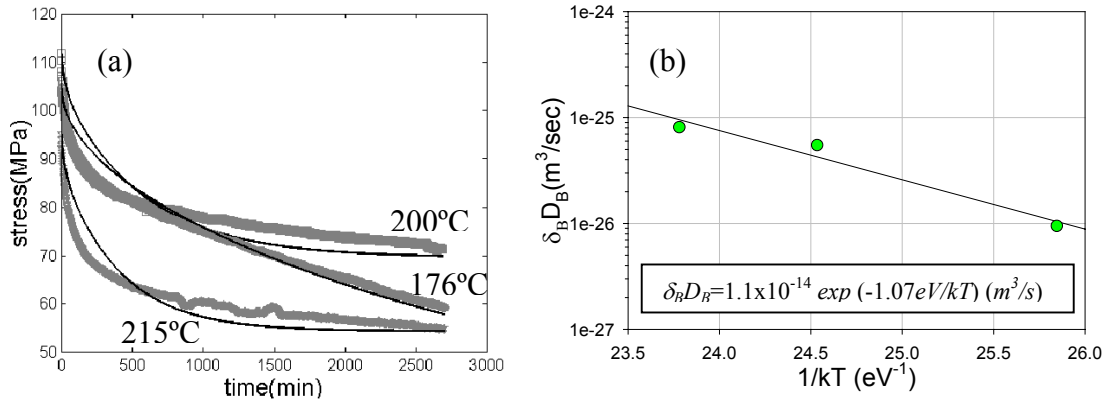

FIGURE 6. Deduction of the grain boundary diffusivities from the stress relaxation measurements: (a) experimental data and the fitting by the diffusion model (Eq. 6); (b) the deduced grain boundary diffusivity as a function of temperature.

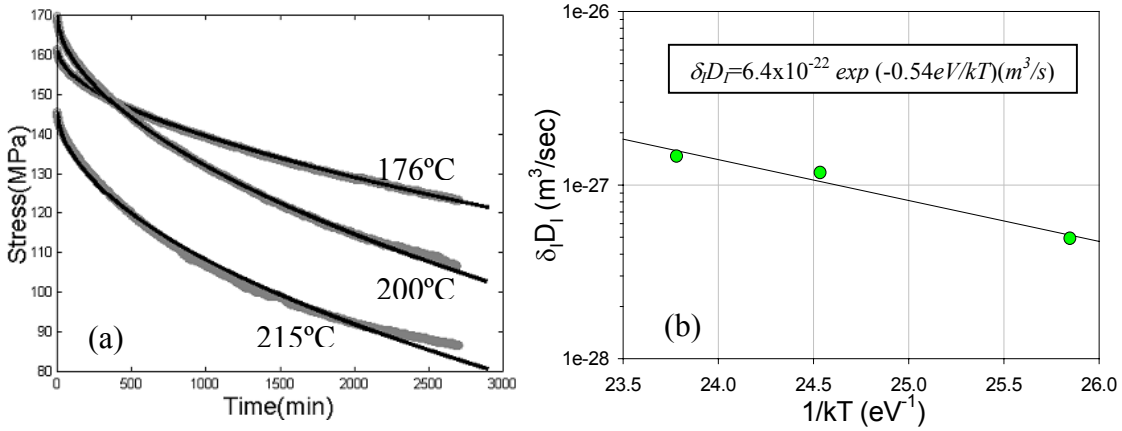

FIGURE 7. Deduction of the Cu/SiN interface diffusivity from the stress relaxation measurement: (a) experimental data and the fitting by the coupled diffusion model (numerical solutions); (b) the deduced Cu/SiN interface diffusivity as a function of temperature.

interface diffusivity and the grain boundary diffusivity. The grain boundary diffusivity deduced above was used to determine the interface diffusivity. Figure 7(a) shows the stress relaxation curves of the passivated Cu film at 176ºC, 200ºC and 215ºC and the fitting results. A finite difference method was used to obtain the numerical solutions for the coupled diffusion model. Alternatively, Eq. 7 may be used to deduce the interface diffusivities without knowing the grain-boundary diffusivity, under the assumption that the interface diffusion is much slower than the grain boundary diffusion. The deduced interface diffusivities were shown in Fig. 7(b), from which we obtain the activation energy and the pre-exponential factor for the interface diffusion: Q_I = 0.54eV and $\delta_I D_{I0}$ = 6.4 × 10^{-22} m^3/s. In the temperature range of the present study, the deduced Cu/SiN interface diffusivity is about two orders of magnitude smaller than the deduced grain boundary diffusivity.

TABLE 1. Parameters for the Cu films in the present study.

Film thickness (h)	1.0μm
Grain size (l)	1.3μm
Bi-axial modulus (M)	160MPa
Pre-exponential grain boundary diffusivity ($\delta_B D_{B0}$)	1.1×10^{-14}m^3/s
Activation energy for grain-boundary diffusion (Q_B)	1.07eV
Atomic volume (Ω)	1.18×10^{-29}m^3
Boltzmann constant (k)	8.617×10^{-5} eV/K

Some previous studies of Cu films have assumed the same grain boundary diffusivity as in bulk Cu, for which the activation energy is 1.08eV [17]. Other studies have reported different diffusivities for Cu films. For example, Gupta et al [18] reported that Q_B = 0.95eV and $\delta_B D_{B0} = 2.9 \times 10^{-15}$ m^3/s. Comparing to these results, the grain boundary diffusivity and the activation energy extracted in the present study seems to be reasonable. For the interface diffusivity, we are not aware of any previous report. In sub-micron Cu lines with bamboo-like microstructures, the Cu/cap layer interface is believed to be the dominant diffusion path for electromigration (EM) and the correlated activation energy was found to be in the range of 0.8eV to 1.2eV [1]. Obviously, the activation energy, 0.54eV, deduced in this study is lower than the values measured by the EM test. Reasons for this discrepancy may relate to the properties of the interface in the passivated Cu film used in this study. EM lifetime is controlled by the mechanism of damage formation, a complex process where the diffusivity is only one of the controlling factors. It may not be surprising that the EM activation energy differs from that for interface diffusion.

As shown in Figs. 6 and 7, the agreement between the experiments and the model is reasonably good for both unpassivated and passivated Cu films. Relatively large discrepancy is noted at the initial stage of stress relaxation, especially for the unpassivated film. This may be attributed to the uncertainties in the transient behavior when the initial stress distribution is not well quantified and other deformation mechanisms may also contribute. The effect is less significant in the passivated film, resulting in a better agreement in Fig. 7(a).

CONCLUDING REMARKS

In this study, stresses in passivated and unpassivated electroplated Cu films were measured under thermal cycling and isothermal annealing at selected temperatures. Thermal cycling experiments showed the effect of passivation, resulting in reduced plastic deformation and higher residual stresses in the passivated film. However, isothermal stress relaxation measurement is more suited for the study of mass transport. A coupled diffusion model was developed to quantitatively correlate the isothermal stress relaxation with the kinetics of mass transport. Based on the diffusion model, both grain boundary and interface diffusivities were deduced from the isothermal stress relaxation measurements in the unpassivated and passivated Cu

films. It was found that the Cu/SiN interface diffusivity is considerably smaller than the grain boundary diffusivity at the temperature range of the present study. Similar measurements and analyses can be applied to other cap layers, which provides an effective method to evaluate the effect of passivation on interfacial mass transport and EM reliability of Cu interconnects.

While the coupled diffusion model captures essential features of the isothermal stress relaxation experiments in electroplated Cu films, we caution that the model should be used within a certain range of temperatures and stresses when the considered diffusion mechanism dominates the deformation process. When the initial stress is high or the temperature is high, other deformation mechanisms such as dislocation glide and power-law creep may intervene the diffusion process and even dominate the stress relaxation. It may be possible to determine the proper temperature-stress range for a particular deformation mechanism through a systematic study of isothermal stress relaxation at various temperatures and stress levels so as to construct a deformation mechanism map similar to those for bulk materials [17]. In addition, a better understanding is needed for the significant zero-creep stress observed in the experiments and the transient behavior of stress relaxation especially for the unpassivated films.

ACKNOWLEDGMENTS

This work was in part supported by Advanced Technology Program of Texas Higher Education Coordinating Board and Intel Corporation.

REFERENCES

1. Hu, C.K., Rosenberg, R., and Lee, K.Y., *Appl. Phys. Letters* **74**, 2945 (1999).
2. Besser, P., Marathe, A., Zhao, L., Herrick, M., Capasso, C. and Kawasaki, H., IEDM, Technical Digest, Piscataway, NJ, 119 (2000).
3. Lane, M.W., Liniger, E.G., and Lloyd, J.R., *J. Appl. Phys*. **93**, 1417 (2003).
4. Hu, C.K., Gignac, L., Rosenberg, R., Liniger, E., Rubino, J., Sambucetti, C., Domenicucci A., Chen, X., and Stamper, A.K., *Appl. Phys. Letters*. **81**, 1782 (2002).
5. Bower, A.F., Singh, N., Gan, D., Yoon, S., Ho, P.S., Leu, J., Shankar, S., *J. Appl. Phys*., in press.
6. Yeo, I.-S., PhD dissertation, University of Texas at Austin, 1996.
7. Flinn, P.A., *J. Mater. Res*. **6**, 1498 (1991).
8. Thouless, M.D., Gupta, J., and Harper, J.M.E., *J. Mater. Res*. **8**, 1845 (1993).
9. Vinci, R.P., Zielinski, E.M., and Bravman, J.C., *Thin Solid Films* **262**, 142 (1995).
10. Gan, D.W., PhD dissertation, University of Texas at Austin, 2004.
11. Keller, R.M., Baker, S.P., Arzt, E., *J. Mater. Res*. **13**, 1307 (1998).
12. Frost, H.J., *Mat. Res. Soc. Symp. Proc*. **265**, 3 (1992).
13. Josell, D., Weihs, T.P., and Gao, H., *MRS Bulletin* **27**, 39 (2002).
14. Mullins, W.W., *J Appl Phys* **28**, 333 (1957).
15. Guduru, P.R., Chasen, E., Freund, L.B., *J. Mech. Phys. Solids* **51**, 2127 (2003).
16. Gao,H.J., Zhang, L., Nix, W.D., Thompson, C.V. and Arzt, E., *Acta Mater*. **47**, 2865 (1999).
17. Frost, H.J., and Ashby, M.F., *Deformation-Mechanism Maps*, New York, Pergamon Press Inc, 1982, p54
18. Gupta, D., Hu, C.-K., and Lee, K.L., *Defect and Diffusion Forum*, **143-147**, 1397 (1997).